12-11-2023

Evaluation of Various Turbulence Models for Turbulent Separated Flow over a Model Two-dimensional Bump

Xuehui Qian
Washington University in St. Louis

E37 MEMS 500 09 – Independent Study

Evaluation of Various Turbulence Models for Turbulent Separated Flow over a Model Two-dimensional Bump

Xuehui Qian[1] and Ramesh K. Agarwal[2]
Washington University in St. Louis, St. Louis, MO 63130

In this paper, performance of several turbulence models is evaluated by computing the turbulent separated flow over a 2D bump using the RANS equations. The turbulence models considered are the Spalart-Allmaras (SA), SST k-ω, and Wray-Agarwal (WA) models. The geometry of the 2D bump is the centerline geometry of the NASA/Virginia Tech (VT) 3D BeVERLI hill bump. Since the experimental data is available only for the 3D bump, the goal of this paper is to compare the numerical solutions using the three turbulence models on a series of grids from coarse to fine. The experimental data of the 3D bump is also presented to evaluate the trends in the predicted pressure and velocity fields of the 2D bump. Three cases with three different freestream Reynolds numbers are computed. The surface pressure coefficients on the 2D bump and the velocity vectors are computed in the computational domain surrounding the 2D bump. The Wray-Agarwal model predicts results with similar trends as the 3D experimental data and gives results consistent with the other two models, which gives confidence in using the WA model for computing the turbulent separated flows. In addition, the WA model results show better agreement with the SST k-omega model results compared to the results from the Spalart-Allmaras model, which indicate good accuracy of the WA model. This paper presents an additional carefully generated test case for the turbulence modeling community for testing the turbulence models for turbulent separated flows.

Nomenclature

s	=	Squared top width
w	=	Bump width
H	=	Bump height
y^+	=	Dimensionless wall distance for the first mesh layer
Re_H	=	Bump-height based Reynolds number
$P_{0,in}$	=	Stagnation pressure at the inlet
$T_{0,in}$	=	Stagnation temperature at the inlet
P_{out}	=	Outlet static pressure
U_∞	=	Freestream velocity
ρ_∞	=	Freestream density
M_∞	=	Freestream Mach number
μ_t/μ	=	Inflow viscosity ratio
x/H	=	X Cartesian position variable normalized by the bump height
$C_{p,ref}$	=	Reference pressure coefficient

[1] Master's student, Mechanical Engineering & Material Science

[2] William Palm Professor of Engineering, Dept. Mechanical Engineering & Material Science, Fellow AIAA

I. Introduction

The NASA/Virginia Tech BeVERLI Hill bump is a three-dimensional geometry which represents the turbulent separated flow. Wind tunnel tests have been conducted to describe the characteristics of the flow and have produced detailed experimental data to meet the requirements of a CFD verification/validation test case as described by Oberkampf and Smith [1]. However, there is no experimental data for the two-dimensional version of the NASA/ Virginia Tech bump considered in this paper. Therefore, three turbulence model are employed to provide the high-quality numerical data for the separated flow field over the two-dimensional version of the NASA/Virginia Tech bump using the Reynolds-Averaged Navier-Stokes (RANS) equations in conjunction with the Spalart-Allmaras (SA) [2], SST k-ω [3], and Wray-Agarwal (WA) [4] models at various Reynolds numbers. The computations are conducted using Ansys Fluent by incorporating a user defined function (UDF) for the WA model. The numerical results from the three models are compared and analyzed to assess the performance of the WA model with respect to the other two models.

II. Geometry Setup

The geometry of the three-dimensional NASA/Virginia Tech bump is defined by Gargiulo et ta. [5]. It has a square flat top, four super elliptic corners and a 5th degree polynomial centerline profile that could be described by the equation [6]:

$$z(x) = P_5(x) = a_5x^5 + a_4x^4 + a_3x^3 + a_2x^2 + a_1x^1 + a_0, \qquad x \in \left[\frac{s}{2}, \frac{w}{2}\right] \ (in) \tag{1}$$

where a_5= -35.46e-6, a_4=1.79e-3, a_3=-25.21e-3, a_2=121.49e-3, a_1=-203.22e-3, and a_0=7.48. The squared top width *s* and the bump width *w* are 0.093472 m and 0.93472 m respectively, and the height of the bump is 0.186944 m. For the two-dimensional bump geometry, the profile along the centerline of the three-dimensional bump is selected, which consists of a flat top and a 5th degree polynomial centerline profile. The geometry is generated using the Computer-Aided Design (CAD) and Ansys Design Modeler. The 2D bump geometry is shown in Figure 1.

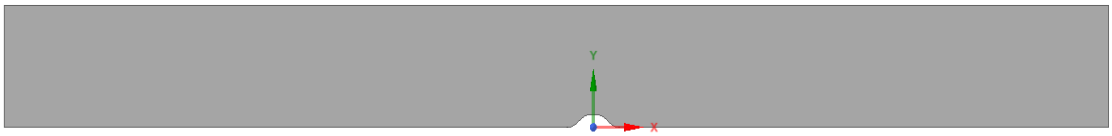

Fig. 1: Geometry of the two-dimensional bump

III. Computational Domain and Mesh Generation

The computational domain is set as a rectangular geometry as shown in Fig. 2. To be consistent with the wind tunnel test for the three-dimensional bump, the computational domain of this two-dimensional bump is extended by 6.5 m and 5.5 m in the negative and positive x- directions, respectively. In addition, the height of the domain is 1.83 m. This size of the computational domain not only makes it possible to model the inflow boundary layer correctly but also makes sure that the flow will not be influenced by the outlet domain.

Structured grids are generated with Ansys ICEM software inside the computational domain. The domain boundaries are labeled as inlet, outlet, top wall and bottom wall, respectively. The y^+ of the first mesh layer from the bump is ensured to be less than one so that accurate results could be obtained using all the turbulence models. Figure 2 shows the structured mesh inside the computational domain.

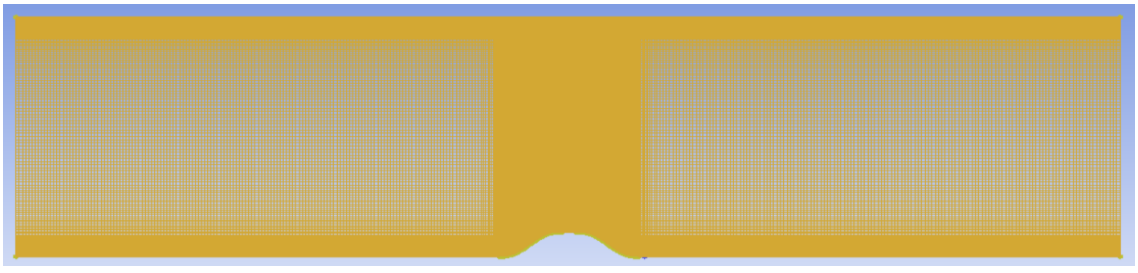

Fig. 2 Structured mesh inside the computational domain for the two-dimensional bump.

IV. Boundary Conditions

Three cases with different bump-height-based Reynolds numbers are studied in this paper. Detailed boundary conditions of the three cases are listed in Table 1 [7]. The boundary conditions are obtained experimentally. The reference pressure P_{ref} is obtained at -2.223 m upstream of the bump and is used to calculate the pressure coefficient. In addition, no-slip boundary conditions are applied on the walls. The flow over this two-dimensional version of the NASA/Virginia Tech (VT) bump is regarded as compressible ideal gas whose dynamic viscosity is defined by the Sutherland's law.

Table 1. Boundary Conditions

Re_H	Re_H = 250K	Re_H = 325K	Re_H = 650K
$P_{0,in}$ (Pa)	94220	94275	94450
$T_{0,in}$ (K)	297	94275	297
P_{out} (Pa)	93961	297	92692
U_∞ (m/s)	21.11	93845	55.22
ρ_∞ (kg/m^3)	1.1031	27.23	1.0930
M_∞	0.0611	1.1023	0.1603
P_{ref} (Pa)	93974	0.0789	92771
T_{ref} (K)	296.8	93866	295.5
μ_t/μ	1.5	296.6	3

V. Results

It should be noted that all the results presented in this section are grid independent, The details of the solutions on various grids from coarse to fine will be included in the complete paper to be presented at the time of the conference.

A. Pressure Distribution Predictions

Figures 3 - 5 show the variation in the surface pressure coefficient with *x*/*H*, where *H* is the bump height which varies for the three cases with three different Reynolds numbers. The reference pressure mentioned in Table 1 is used to compute the pressure coefficient, which is calculated by the following equation [7]:

$$C_{p,ref} = \frac{P - P_{ref}}{\frac{\gamma}{2} * P_{ref} * M_\infty^2} \tag{2}$$

In each figure, the predictions of pressure coefficients obtained using the three turbulence models are presented for a given Reynolds number. In addition, for cases with Reynolds numbers *Re* = 250,000 and 650,000, the experimental data for the corresponding three-dimensional bump is also included to show the three-dimensional effect. Similar trends in the pressure distributions for the three-dimensional bump and the two-dimensional bump indicate the correctness of the 2D numerical predictions.

Figure 3 shows the results for the case with Re = 250,000, all the three models show excellent agreement upstream of the bump until *x/H* = -0.5, when the flow approaches the flat top of the bump. After this location, while the results from WA model and the SST k-omega model show good agreement with each other, the SA model predicts slightly lower values of the pressure coefficient compared to the WA and SST k-omega models until close to *x/H* = 1. It should be noted that although the WA model and the SST k-omega model predict similar results, they begin to show differences as the flow move towards the downstream direction. As the flow travels downstream, the differences become larger and larger. After *x/H* = 1, the WA model shows agreement with the SA model over a short distance; however, all the three models vary in the prediction downstream of *x/H* = 1. All the three models predict results with similar trend as the three-dimensional experimental data again attesting to the correctness of the numerical predictions for the 2D bump.

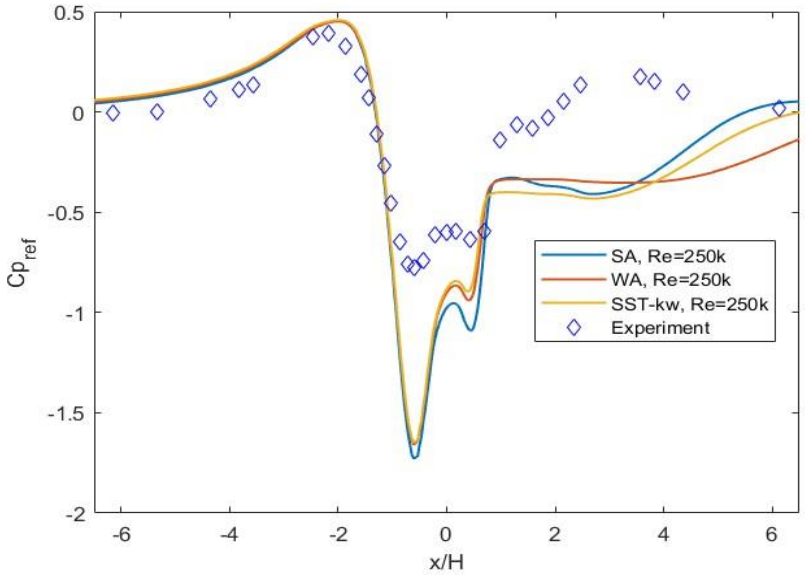

Fig. 3 Variation in computed pressure coefficients with distance *x/H* along the 2D bump at *Re* = 250,000 using the SA, WA, and SST k-omega models, and their comparison with the corresponding experimental data for the 3D bump.

Figure 4 shows the case with *Re* = 325,000. This case shows similar trend in the results for *Re* = 250,000, the computations from all the three models are consistent with each other until the flow approaches the flat top of the bump, after that the SA model predicts the lowest value while the results from the other two models are very close to each other. After x/H = 1, the results predicted by all the three models vary.

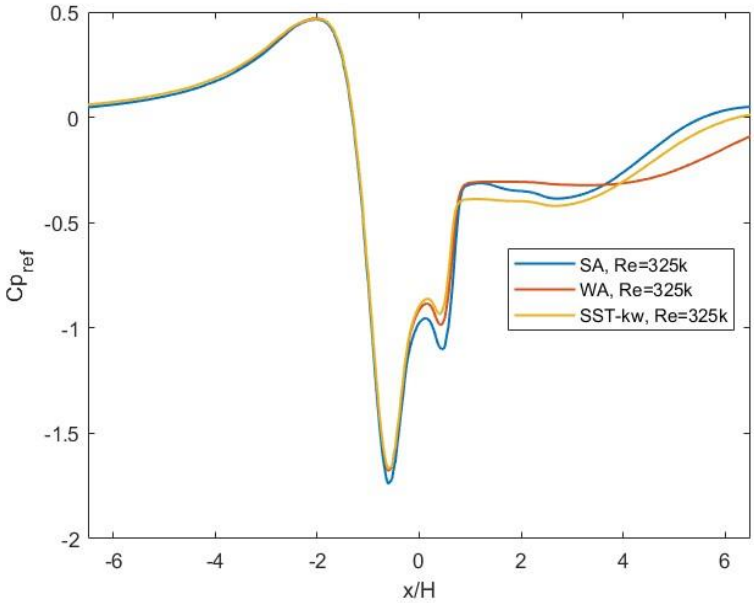

Fig. 4 Variation in computed pressure coefficients with distance *x/H* along the 2D bump at *Re* = 325,000 using the SA, WA, and SST k-omega models.

Figure 5 shows the results for *Re* = 650,000 case. Although the overall results show similar trends as in the previous two cases, in this case the prediction from the SA model differs from the other two models with higher values in the upstream region until close to *x/H* = -2, when the flow reaches the bump. The SA model prediction has the highest value compared to the other two models in majority of the flow domain except shows agreement with the results from the other two models in the region between the bump boundary and

the flat top. Again, the results from the WA model and the SST k-omega model show consistency until close to *x/H* = 1. After that, the predictions from all the three models vary as in the previous two cases. The relationship of the computations for the 2D bump with the trend of the three-dimensional experimental data is the same as for Re = 250,000 case.

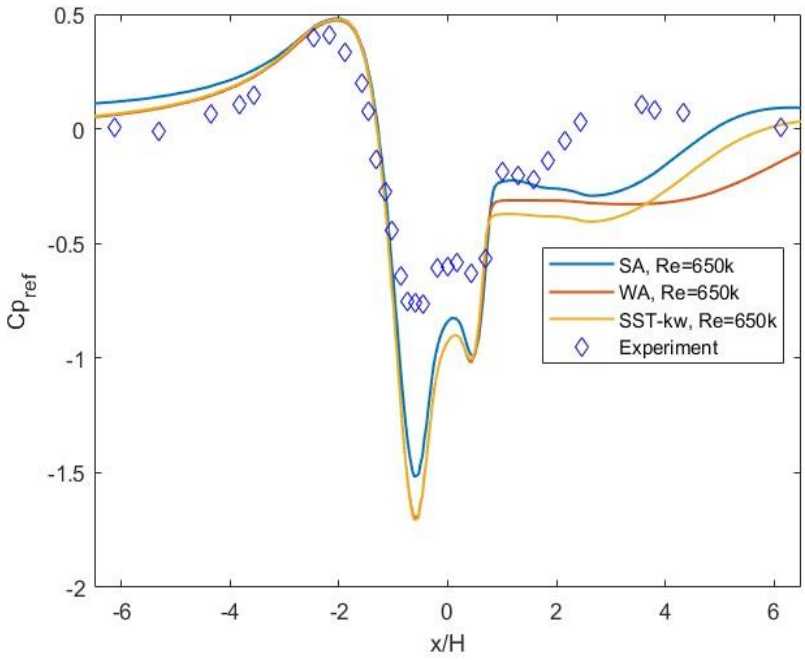

Fig. 5 Variation in computed pressure coefficients with distance *x/H* along the 2D bump at *Re* = 650,000 using the SA, WA, and SST k-omega models, and their comparison with the corresponding experimental data for the 3D bump.

B. Velocity Vectors

To observe the flow over the bump and the separated flow region behind the bump, the velocity vectors in the computational domain are plotted. Figures 6 - 8 show the velocity vectors at *Re* = 250,000, 325,000, and 650,000, respectively. In each of these figures, the plots with velocity vectors using the three different turbulence models are provided. It can be observed that the flow keeps accelerating as it moves downstream and reaches the maximum velocity at the flat top of the bump. A separated flow region can be observed at all three Reynolds numbers using all the three turbulence models. It can be noted that compared to the WA model and the SST k-omega model, the SA model predicts a smaller separation region.

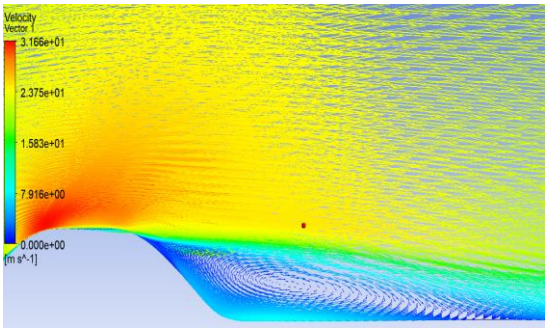

(A)

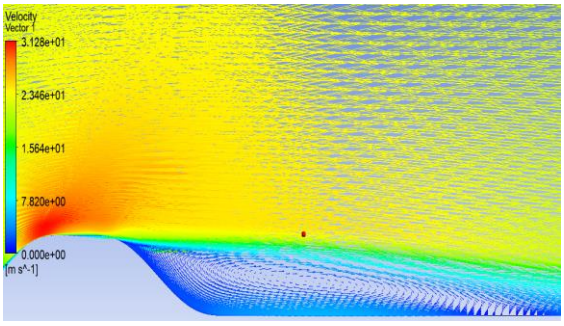

(B)

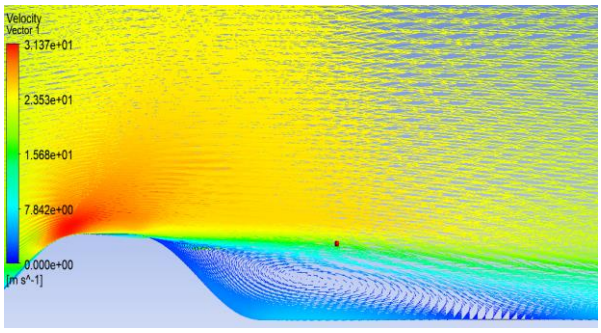

(C)

Fig. 6 Velocity vectors in the computational domain of 2D bump at *Re* = 250,000 using the (A) SA model, (B) WA model, and (C) SST k-omega model.

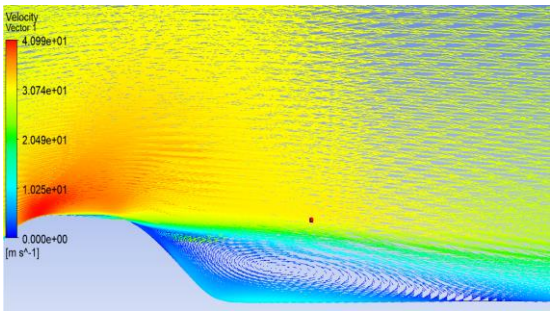

(A)

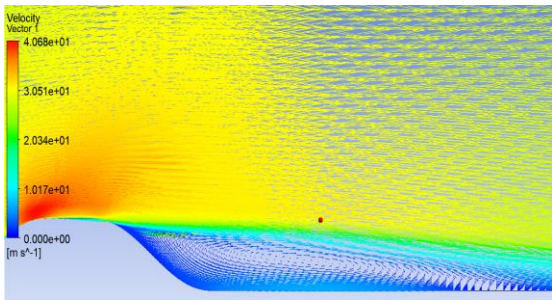

(B)

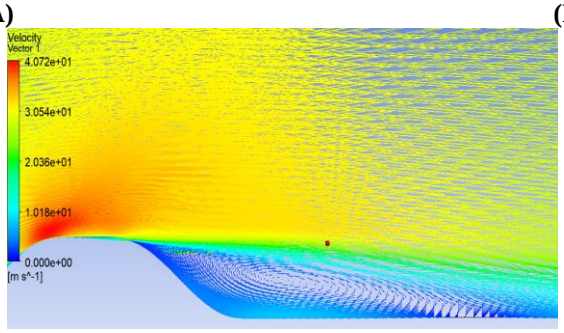

(C)

Fig. 7 Velocity vectors in the computational domain of 2D bump at *Re* = 325,000 using the (A) SA model, (B) WA model, and (C) SST k-omega model.

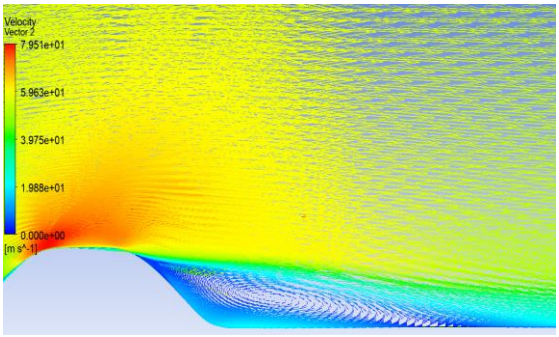

(A)

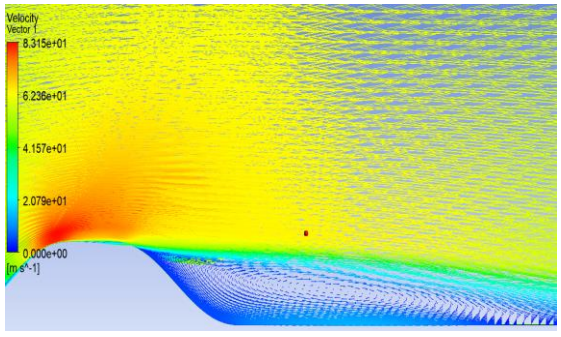

(B)

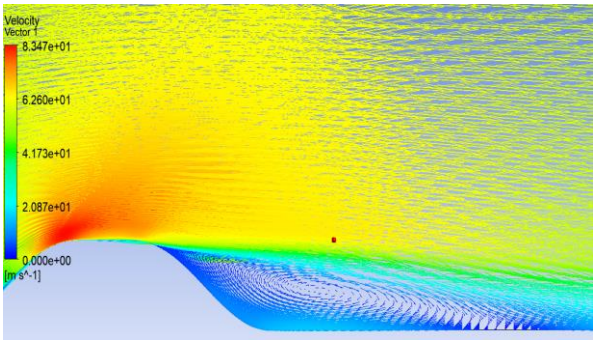

(C)

Fig. 8 Velocity vectors in the computational domain of 2D bump at *Re* = 650,000 using the (A) SA model, (B) WA model, and (C) SST k-omega model.

VI. Conclusions

The computations are performed for the separated flow field over the two-dimensional version of the NASA/Virginia Tech (VT) bump using the Reynolds-Averaged Navier-Stokes (RANS) equations in conjunction with the Spalart-Allmaras (SA), the SST k-ω, and the Wray-Agarwal (WA) models at various Reynolds numbers. The goal of this investigation has been to provide high quality numerical data for a carefully created 2D test case for the turbulence modeling community for testing the turbulence models for turbulent separated flows. The 2D results for pressure coefficient using all three turbulence models are also compared with the 3D results for the pressure coefficients, similar trends can be observed in both the 2D and 3D results although their magnitudes are expected to be different; the 3D results have lower magnitude due to three-dimensional effects. The velocity vectors in the computational domain are also plotted to determine the separation region behind the bump. The separation regions computed by the SST k-ω, and the Wray-Agarwal (WA) models are very close to each other; however, the Spalart-Allmaras (SA) model predicts a slightly smaller separation zone affecting the location of separation and reattachment points.

References

[1] Oberkampf, W. L., and Smith, B. L., "Assessment Criteria for Computational Fluid Dynamics Model Validation Experiments,' Journal of Verification, Validation and Uncertainty Quantification, Vol. 2, No. 3, 2017, p. 031002.

[2] Spalart, P. and Allmaras. S., "A One-Equation Turbulence Model for Aerodynamic Flows," AIAA Paper 1992-439, 30th Aerospace Sciences Meeting and Exhibit, Reno, NV, 1992, https://doi.org/10.2514/6.1992-439.

[3] Menter, F. R., "Two-Equation Eddy-Viscosity Turbulence Models for Engineering Applications," AIAA Journal, Vol. 32, No. 8, August 1994, pp. 1598-1605, https://doi.org/10.2514/3.12149.

[4] Han, X., Rahman, M. M., and Agarwal, R. K., "Development and Application of a Wall Distance Free Wray-Agarwal Turbulence Model," AIAA Paper 2018-0593, AIAA SciTech Forum, Kissimmee, FL, 8-12 January 2018

[5] Gargiulo, A., Beardsley, C., Vishwanathan, V., Fritsch, D. J., Duetsch-Patel, J. E., Szoke, M., Borgoltz, A., Devenport, W. J., Roy, C. J., and Lowe, K. T., "Examination of Flow Sensitivities in Turbulence Model Validation Experiments," AIAA SciTech 2020 Forum, 2020.

[6] Lowe, T., Borgoltz, A., Devenport, W. J., Fritsch, D. J., Gargiulo, A., Duetsch-Patel, J. E., Roy, C. J., Szoke, M., and Vishwanathan, V., "Status of the NASA/Virginia Tech Benchmark Experiments for CFD Validation," AIAA SciTech 2020 Forum, 2020.

[7] Ozoroski, T. A., "Overview of the Computational Fluid Dynamics Analyses of the Virginia Tech/NASA BeVERLI Hill Experiments," M.S. thesis, Virginia Tech., 2022.